

Available online at www.sciencedirect.com

Polar Science 3 (2010) 222–234

NIPR
National Institute of Polar Research<http://ees.elsevier.com/polar/>

Titanium behavior in quartz during retrograde hydration: Occurrence of rutile exsolution and implications for metamorphic processes in the Sør Rondane Mountains, East Antarctica

Tatsuro Adachi ^{a,*}, Tomokazu Hokada ^{a,b}, Yasuhito Osanai ^c, Tsuyoshi Toyoshima ^d,
Sotaro Baba ^e, Nobuhiko Nakano ^c

^a Department of Polar Science, School of Multidisciplinary Sciences, The Graduate University for Advanced Studies, 10-3 Midori-cho, Tachikawa, Tokyo 190-8518, Japan

^b National Institute of Polar Research, 10-3 Midori-cho, Tachikawa, Tokyo 190-8518, Japan

^c Division of Evolution of Earth Environments, Faculty of Social and Cultural Studies, Kyushu University, 744 Motoooka, Nishi-ku, Fukuoka 819-0395, Japan

^d Graduate School of Science and Technology, Niigata University, 8050 Ikarashi 2-no-cho, Niigata-shi, Niigata 950-2181, Japan

^e Department of Natural Environment, University of the Ryukyus, 1 Senbaru, Nishihara, Okinawa 903-0213, Japan

Received 15 May 2009; revised 19 August 2009; accepted 24 August 2009

Available online 14 October 2009

Abstract

In the central Sør Rondane Mountains, East Antarctica, orthopyroxene felsic gneiss (OPG) was converted to hornblende-biotite felsic gneiss (HBG) by hydration that accompanied the intrusion of pegmatite. The retrograde HBG contains exsolved rutile in quartz. The composition of orthopyroxene and clinopyroxene in OPG suggests a temperature of 840 °C (interpreted as the near-peak temperature), and the composition of hornblende and plagioclase in HBG suggests a temperature of 670–700 °C (interpreted as the temperature during hydration). Ti concentrations in quartz were measured using an electron probe micro-analyzer, and Ti-in-quartz thermometers were applied. Measured Ti concentrations were 110 ppm (equivalent to 760–820 °C) for homogeneous quartz from OPG and 35 ppm (650–700 °C) for an exsolution-free area of a quartz grain from HBG. The pre-exsolution Ti concentration in quartz from HBG was reconstructed with 100 μm beam diameter and 25 kV of accelerating voltage, giving 103 ppm, similar to the value obtained for homogeneous quartz in OPG. The temperatures obtained using a Ti-in-quartz thermometer are consistent with those estimated using other thermometers. Although analysis of the main constitute minerals in HBG yields the conditions of hydration, the reconstructed pre-exsolution Ti content in quartz within HBG yields the pre-hydration conditions. Thus, the Ti-in-quartz thermometer is a potentially powerful tool with which to identify the peak or near-peak temperature conditions, even for retrogressed metamorphic rocks.

© 2009 Elsevier B.V. and NIPR All rights reserved.

Keywords: Rutile exsolution; Ti-in-quartz thermometer; Granulite; Hydration retrograde metamorphism; Sør Rondane Mountains

* Corresponding author. 10-3 Midori-cho, Tachikawa, Tokyo 190-8518, Japan.

E-mail address: t-adachi@nipr.ac.jp (T. Adachi).

1. Introduction

Recent experimental studies have noted the temperature dependence of Ti solubility in quartz. Wark and Watson (2006) and Kawasaki and Osanai (2008) developed calibrated Ti-in-quartz thermometers that enable estimates of the temperature conditions of igneous and metamorphic rocks. In high-temperature metamorphic terranes, rutile exsolution is commonly observed in silicate minerals such as quartz, garnet, orthopyroxene, sapphirine, K-feldspar, and osumilite (e.g., Osanai et al., 2001; Osanai and Yoshimura, 2002). Rutile exsolution is generally considered to occur when a Ti-rich precursor precipitates excess Ti in response to decreasing Ti solubility during cooling or decompression (e.g., Kawasaki and Motoyoshi, 2007; Zhang et al., 2003). Accordingly, the chemical composition of pre-exsolution quartz probably preserves a record of metamorphism prior to the final equilibrium conditions.

The Sør Rondane Mountains, East Antarctica, is a high-grade metamorphic terrane that contains voluminous late-stage igneous rocks (e.g., Kojima and

Shiraishi, 1986). The area is subdivided into the Northeastern and Southwestern terranes, with the former containing orthopyroxene-bearing metamorphic rocks (Osanai et al., 1992). However, the orthopyroxene-bearing gneisses are commonly surrounded by orthopyroxene-free gneisses. Moreover, in large parts of the Northeastern Terrane, felsic and pelitic rocks are strongly retrogressed, resulting in modification to the original mineral assemblages and chemical compositions attained at the peak metamorphic conditions. This overprinting makes it difficult to recognize the primary distribution of granulite in the Sør Rondane Mountains. We found rutile exsolution in the retrograde rocks that are widespread throughout the Northeastern Terrane (Fig. 1). The exsolution probably indicates an early high-grade metamorphic event; consequently, it may represent a key in understanding the granulite metamorphism observed in the Sør Rondane Mountains.

In this study, we investigate orthopyroxene felsic gneiss (OPG) and hornblende-biotite felsic gneiss (HBG) collected from the same outcrop, where HBG occurs as a narrow 1–2 m zone at the boundary between OPG and a pegmatite intrusion. We propose

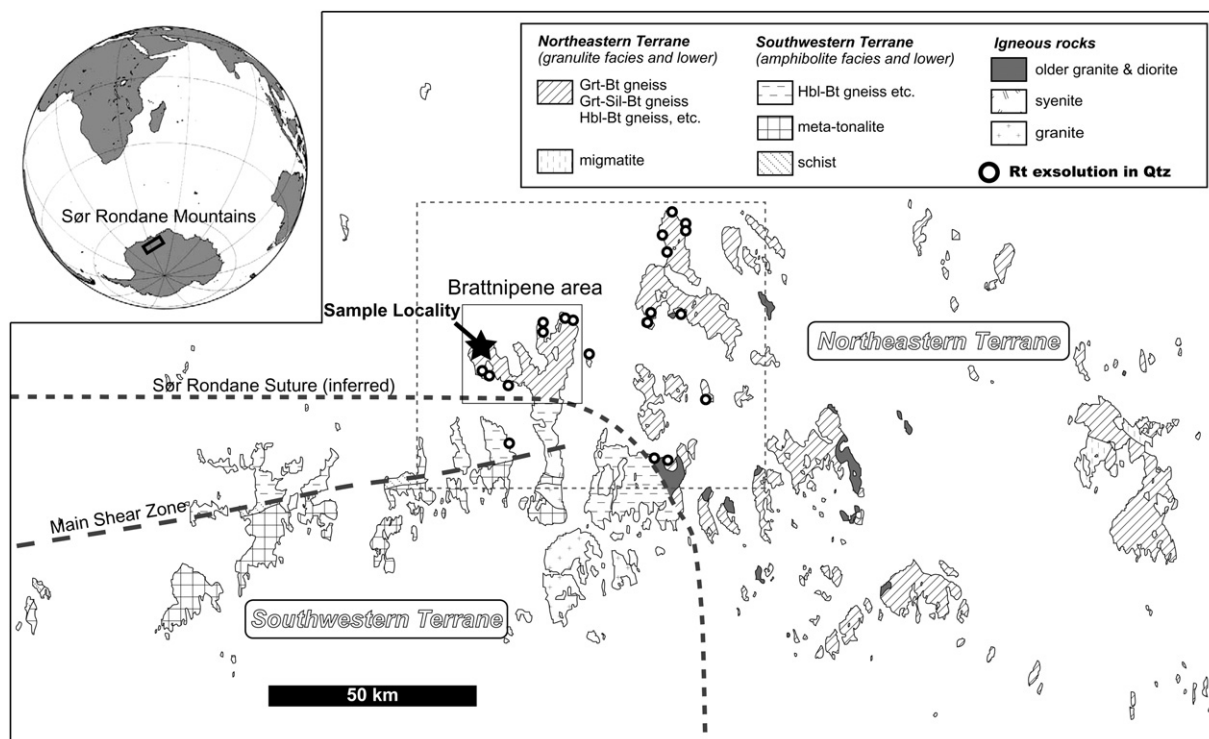


Fig. 1. Geological map of the Sør Rondane Mountains (modified after Shiraishi et al., 1997). The sample locality is marked with a star. The location of the Sør Rondane Suture follows that proposed by Osanai et al. (1992). The dashed rectangle shows the area investigated in the present study.

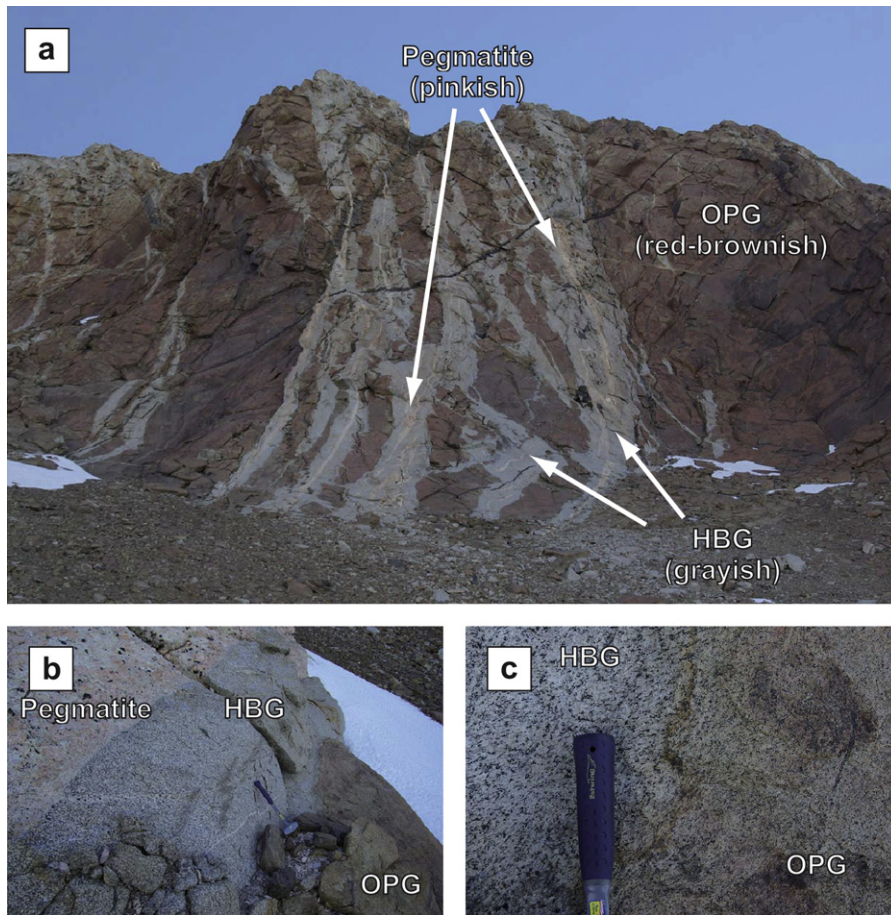


Fig. 2. Photographs of the sampled outcrop. (a) Large-scale field relationships among the studied rocks. Hornblende-Biotite felsic gneiss (HBG; grayish color) occurs within a bleached zone (about 1–2 m wide) in association with pegmatite veins (pinkish color), entirely within orthopyroxene felsic gneiss (OPG; red-brownish color). OPG is never in direct contact with pegmatite. (b) Photograph of the contacts between the three lithologies. (c) Close-up photograph of OPG and HBG. A foliation is continuous between OPG and HBG.

that OPG was converted to HBG by the effects of pegmatite intrusion. Rutile exsolution in quartz is found only in HBG. A comparison of Ti behavior between OPG and HBG, combined with data regarding petrogenetic relationships, enables us to consider those factors that controlled the occurrence of rutile exsolution. We measure Ti concentrations in quartz using an electron probe micro-analyzer (EPMA) and we apply a Ti-in-quartz thermometer to exsolution-free OPG and exsolution-bearing HBG, and discuss the implications of rutile exsolution for metamorphism in this region.

2. Geological outline of the Sør Rondane Mountains

The Sør Rondane Mountains of East Antarctica (22°–28°E, 71.5°–72.5°S) lie within a Latest

Proterozoic to Early Cambrian collision zone, the so-called East African–Antarctic Orogen (EAAO; Jacobs et al., 2003). The mountains are composed of high-grade metamorphic rocks and various plutonic intrusions (Fig. 1). This area is subdivided into the Northeastern and the Southwestern terranes based on lithology and metamorphic grade (Osanaï et al., 1992). The Northeastern Terrane is dominated by amphibolite- to granulite-facies metamorphic rocks of pelitic, psammitic, and felsic compositions. The temperature and pressure conditions recorded by rocks of the Northeastern Terrane are estimated to be 800 °C and 7–8 kbar at peak metamorphism, and 530–580 °C and 5.5 kbar during subsequent amphibolite-facies retrograde metamorphism (e.g., Asami and Shiraishi, 1987; Shiraishi and Kojima, 1987). The Southwestern Terrane is composed mainly of greenschist- to amphibolite-facies metamorphic rocks of felsic and

intermediate compositions. The metamorphic conditions of the Southwestern Terrane are estimated to be those of the upper amphibolite facies, followed by retrogression and accompanying mylonitization (Shiraishi and Kojima, 1987).

3. Field relationships

Samples of OPG (sample 07121003A) and HBG (sample 07121003B) were collected from the Koyubi Ridge in the western part of the Brattnipene area in the Sør Rondane Mountains. At this outcrop, the host rock, brownish OPG, is intruded by K-feldspar–plagioclase–quartz–mica pegmatite (Fig. 2a). These two rock types are not in direct contact, as grayish HBG occurs along the OPG–pegmatite boundary (Fig. 2b). A foliation, oriented oblique to the lithological boundary, is continuous from OPG to HBG (Fig. 2c). Based on these observations, it can be interpreted that HBG is the hydrated (bleached) equivalent of OPG.

Shiraishi and Kagami (1992) reported a similar relationship at a neighboring outcrop in the Brattnipene area. The authors reported Sm–Nd and Rb–Sr ratios of orthopyroxene-bearing enderbite gneisses and bleached hornblende-biotite-bearing felsic gneisses. Sm–Nd and Rb–Sr isochrones for whole-rock samples of the two lithologies yielded ages of 978 ± 52 Ma and 961 ± 101 Ma, respectively. Shiraishi et al. (2008) reported zircon U–Pb ages from the enderbite gneisses: 951 ± 17 Ma from oscillatory zoned prismatic cores and 602 ± 15 Ma from unzoned rims, interpreted as the timing of magmatism of the protolith and granulite facies metamorphism, respectively.

4. Petrography, whole-rock chemistry, and mineral chemistry

4.1. Petrography and mineral chemistry

The mineral assemblages within the analyzed samples are listed in Table 1. Mineral compositions were analyzed using an EPMA (JEOL JXA-8200) with a 5 ch wavelength-dispersive X-ray analytical system (WDS), as installed at the National Institute of Polar Research, Japan. Representative mineral compositions are listed in Table 2. The analyses were performed at 15 kV accelerating voltage, 12 nA probe current, and 2 μ m probe diameter. Mineral abbreviations are after Kretz (1983), and amphibole nomenclature is after Leake et al. (1997).

4.1.1. Orthopyroxene felsic gneiss

OPG (sample 07121003A) is composed mainly of quartz, plagioclase, orthopyroxene, clinopyroxene, hornblende, biotite, ilmenite, and magnetite, with accessory apatite and zircon. Orthopyroxene ($X_{Mg} = 0.41$) makes up a large portion of the mafic minerals in OPG (Fig. 3a). Orthopyroxene grains are up to 1 mm in diameter. Clinopyroxene ($X_{Mg} = 0.55$) is 300–500 μ m in size, and is present in the matrix. Hornblende ($X_{Mg} = 0.37$, $TiO_2 = 2.1$ wt%) is brownish, classified as ferro-pargasite, and 0.5–1 mm in size. Biotite ($X_{Mg} = 0.41$, $TiO_2 = 4.2$ wt%) is rare and relatively fine grained (<300 μ m). Plagioclase (1–3 mm) shows antiperthitic texture (Fig. 3b). Host plagioclase is of anorthite–albite solid solution with a minor orthoclase component ($An_{30}Ab_{68}Or_2$), and K-feldspar blebs have a composition of $Or_{95}Ab_5An_{<1}$. Quartz (1–3 mm) contains sparse mineral inclusions (Fig. 3d). Apatite in this sample includes monazite needles with a shape-preferred orientation (Fig. 3b).

Table 1

Mineral assemblages and bulk chemistry for felsic gneisses from the Brattnipene area, Sør Rondane Mountains.

	OPG	HBG	HBG ^b
Qtz	○	○	
Pl	○	○	
Opx	○		
Cpx	×		
Hbl	△	○	
Bt	×	○	
Ep		△	
Ilm	–	–	
Mag	–	–	
Zrn	–	–	
Aln	–	–	
Ap	–	–	
SiO ₂	73.00	70.63	65.84
TiO ₂	0.33	0.39	0.36
Al ₂ O ₃	13.74	14.74	13.74
Fe ₂ O ₃ ^a	3.64	4.46	4.16
MnO	0.07	0.08	0.07
MgO	0.74	0.98	0.91
CaO	3.52	3.92	3.65
Na ₂ O	3.98	4.43	4.13
K ₂ O	1.27	1.01	0.94
P ₂ O ₅	0.08	0.09	0.08
LOI	0.05	0.24	0.22
Total	100.41	100.98	

○, common; △, moderately common; ×, rare; –, accessory.

Mineral abbreviations are after Kretz (1983).

^a Total Fe as Fe₂O₃.

^b Al-normalized value.

Table 2

Representative mineral compositions for felsic gneisses from the Brattnipene area, Sør Rondane Mountains.

Rock type	OPG	OPG	OPG	HBG	HBG	HBG	OPG	HBG	HBG	OPG	HBG	OPG	HBG
Minerals	Opx	Cpx	Hbl	Hbl 1-core	Hbl 1-rim	Hbl 2	Bt	Bt	Ep	Pl	Pl	Kfs bleb	Kfs bleb
SiO ₂	50.35	51.16	40.80	39.95	40.92	41.64	36.20	35.21	38.18	61.19	61.46	63.98	63.70
TiO ₂	0.09	0.17	2.13	2.09	0.76	0.33	4.21	2.58	0.08	0.02	0.01	0.04	0.03
Al ₂ O ₃	0.79	1.64	11.43	11.22	12.36	11.60	14.49	15.22	23.69	24.24	24.04	18.25	18.41
Cr ₂ O ₃	0.02	0.01	0.01	0.00	0.03	0.01	0.02	0.01	0.02	0.01	0.01	0.01	0.01
FeO ^{total}	34.65	14.55	21.56	24.13	24.07	23.39	23.31	25.73	11.21	0.10	0.07	0.03	0.04
MnO	1.30	0.57	0.30	0.49	0.59	0.61	0.14	0.33	0.19	0.02	0.02	0.02	0.02
MgO	13.37	10.01	7.13	5.41	5.66	6.24	8.96	7.44	0.02	0.00	0.00	0.00	0.00
CaO	0.74	21.01	11.08	11.11	11.18	11.61	0.02	0.03	23.31	6.17	5.85	0.04	0.02
Na ₂ O	0.02	0.50	1.39	1.45	1.30	1.04	0.02	0.04	0.00	7.88	8.21	0.52	0.72
K ₂ O	0.01	0.01	1.90	1.85	1.60	1.26	9.62	9.45	0.02	0.39	0.23	15.75	15.25
Total	101.33	99.63	97.73	97.70	98.46	97.72	97.01	96.05	96.71	100.01	99.90	98.64	98.20
Si	1.97	1.97	6.33	6.26	6.28	6.39	5.55	5.52	3.03	2.72	2.73	2.99	2.99
Ti	0.00	0.00	0.25	0.24	0.08	0.04	0.49	0.30	0.00	0.00	0.00	0.00	0.00
Al	0.04	0.07	2.09	2.07	2.24	2.10	2.62	2.81	2.21	1.27	1.26	1.01	1.02
Cr	0.00	0.00	0.00	0.00	0.00	0.00	0.00	0.00	0.00	0.00	0.00	0.00	0.00
Fe ^{3+a}				0.26	0.49	0.58			0.74				
Fe ²⁺	1.14	0.47	2.80	2.90	2.60	2.42	2.99	3.38	0.00	0.00	0.00	0.00	0.00
Mn	0.04	0.02	0.04	0.07	0.08	0.08	0.02	0.04	0.01	0.00	0.00	0.00	0.00
Mg	0.78	0.57	1.65	1.26	1.30	1.43	2.05	1.74	0.00	0.00	0.00	0.00	0.00
Ca	0.03	0.87	1.84	1.86	1.84	1.91	0.00	0.00	1.98	0.29	0.28	0.00	0.00
Na	0.00	0.04	0.42	0.44	0.39	0.31	0.01	0.01	0.00	0.68	0.71	0.05	0.07
K	0.00	0.00	0.38	0.37	0.31	0.25	1.88	1.89	0.00	0.02	0.01	0.94	0.91
Cation Total	4.01	4.01	15.78	15.73	15.61	15.51	15.60	15.71	7.99	4.99	5.00	4.99	4.99
O total	6	6	23	23	23	23	22	22	12.5	8	8	8	8
X _{Mg}	0.41	0.55	0.37	0.30	0.33	0.37	0.41	0.34					
An										0.30	0.28		

^a Fe³⁺ is calculated value. $X_{Mg} = Mg/(Mg + Fe)$, $An = Ca/(Ca + Na + K) \times 100$, $Or = K/(Ca + Na + K) \times 100$.

4.1.2. Hornblende–biotite felsic gneiss

HBG (sample 07121003B) is composed mainly of quartz, plagioclase, hornblende, biotite, ilmenite, and magnetite, with accessory apatite, allanite, and zircon. Hornblende can be divided into two types based on mode of occurrence and composition. Type 1 consists of relatively large grains (up to 2 mm) with $X_{Mg} = 0.30$ and TiO₂ concentrations varying from 2.1 wt% in the core to 0.8 wt% in the rim (Fig. 4a). The mineral color changes from brownish in the core to greenish in the rim. Type 2 consists of a greenish and fine-grained (up to 40 μm) aggregate with quartz, with $X_{Mg} = 0.32$ and TiO₂ < 0.3 wt% (Fig. 4b). Biotite ($X_{Mg} = 0.34$, TiO₂ = 2.6 wt%) shows a radial shape, is 1–2 mm in size, and is commonly in contact with hornblende. The TiO₂ content of biotite in HBG is lower than that in OPG. Plagioclase (1–3 mm) is antiperthite (Fig. 4c). The host plagioclase and K-feldspar blebs have compositions of An₂₈Ab₇₁Or₁ and Or₉₃Ab₇An_{<1}, respectively. The proportion of blebs in HBG appears to be less than that in OPG. Quartz (1–3 mm) contains rutile needles with shape-preferred orientations in three directions (Fig. 4d). The needles, which are less than

1 μm thick and occur throughout the host grains, are interpreted to be of exsolution origin.

4.2. Whole-rock chemistry

Bulk chemical analyses were carried out using a RIGAKU RIX3000 X-ray fluorescence spectrometer installed at the National Institute of Polar Research. The procedures followed in sample preparation and analysis are given in Seno et al. (2002), and the results are listed in Table 1. For HBG, we also present values normalized to Al, which is generally thought to be relatively immobile compared with other elements. As stated above, field relationships indicate that HBG was formed from OPG during intrusion of the pegmatite. The modal abundance of hydrous minerals (including hornblende, biotite, and epidote) in HBG is higher than that in OPG, thereby indicating a supply of fluid from the pegmatite. However, the bulk composition of OPG and the Al-normalized bulk composition of HBG are similar, except for Si, K, and Fe, suggesting that only limited chemical modification resulted from fluid filtration from the pegmatite.

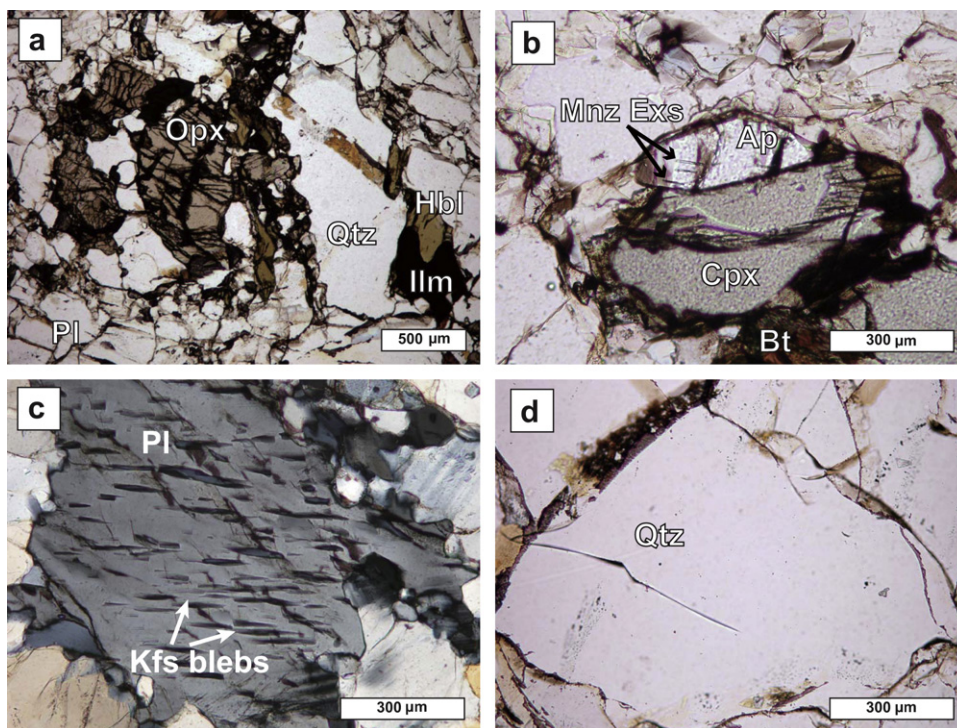


Fig. 3. Photomicrographs of orthopyroxene felsic gneiss (OPG). (a) Mineral relationships in OPG. Orthopyroxene is the main mafic mineral. (b) Occurrence of clinopyroxene and apatite. Clinopyroxene is present in the matrix. Apatite includes monazite needles. (c) Mode of occurrence of plagioclase, showing antiperthitic texture. (d) Quartz in OPG containing scarce mineral inclusions.

5. Measurements of Ti concentrations in quartz

Recent experimental studies have revealed the temperature dependence of the saturated concentration of Ti in quartz (Kawasaki and Osanai, 2008; Wark and Watson, 2006). Wark and Watson (2006) carried out synthetic experiments at temperatures of 600–1000 °C at 1.0 GPa, and Kawasaki and Osanai (2008) calibrated Ti solubility using synthesized quartz at 1300 °C in atmospheric pressure, combined with empirical data for natural quartz. Wark et al. (2007) succeeded in applying this thermometer to natural rhyolite, thereby indicating its applicability at least to felsic rocks such as OPG and HBG. In addition, Kawasaki and Osanai (2008) reported a linear relation between temperature and the logarithm of TiO_2 content in quartz, for several rock types including quartzo-feldspathic rock, Mg-Al rock, and eclogite derived from a mixed pelite–basalt protolith. This finding of a similar relation for different rock types may indicate that the effect of bulk rock chemistry is of little importance, suggesting in turn that Ti-in-quartz thermometers are potentially applicable to a wide range of rock types. According to Wark and Watson (2006), the saturated concentration of Ti in

quartz is 526 ppm ($\text{TiO}_2 = 0.088$ wt%) at 1000 °C, and 140 ppm ($\text{TiO}_2 = 0.023$ wt%) at 800 °C. To quantify such low concentrations of Ti using EPMA requires the selection of an appropriate dispersive crystal, measurement time, and standard for Ti.

5.1. Optimum analytical conditions in analyzing homogeneous domains

Measurements were performed using a JEOL JXA-8200 electron probe micro-analyzer installed at the National Institute of Polar Research, at conditions of 15 kV accelerating voltage, 150 nA probe current, and 2 μm probe diameter.

5.1.1. Dispersive crystal and acquisition time

Quartz in OPG was fully scanned by WDS with normal PET and PETH crystals at acquisition times of 10–50 s (Fig. 5). Compared with normal PET, higher counts of Ti- $K\alpha$ are obtained with PETH; however, a linear baseline cannot be obtained. Because a linear background is essential to obtain precise peak counts, we used a normal PET crystal for Ti analyses. Regarding acquisition time, 50-s measurements at each

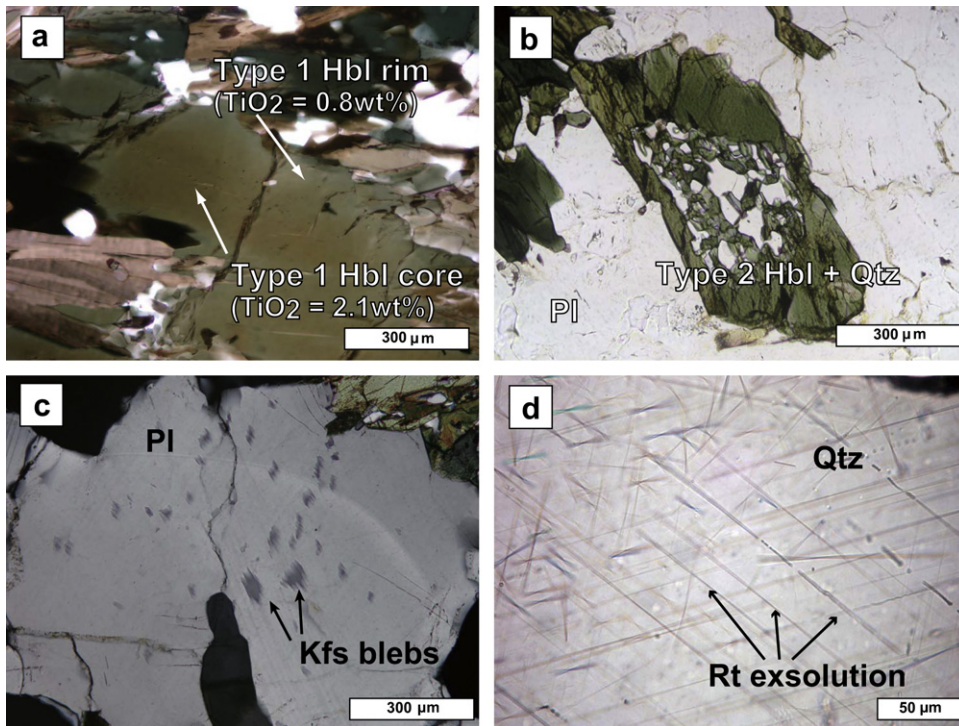


Fig. 4. Photomicrographs of hornblende-biotite felsic gneiss (HBG). (a) Type 1 hornblende shows compositional zoning from a brownish core to a greenish rim. (b) Mode of occurrence of type 2 hornblende, forming an aggregate with quartz. (c) Antiperthitic plagioclase in HBG. The proportion of K-feldspar blebs is less than that in OPG. (d) Rutile exsolution texture in quartz. Rutile needles have a shape-preferred orientation in three directions.

step yield clearer peaks than those obtained using 10-s measurements. For the unknown samples, acquisition time was set to 150 s for both peak and background, which yielded a detection limit of less than 10 ppm.

5.1.2. Standard for Ti

Chromite ($\text{TiO}_2 = 0.120 \text{ wt}\%$), spessartine ($\text{TiO}_2 = 0.108 \text{ wt}\%$), and rutile were considered for use as a standard for Ti, and we assessed the disparity between the reference value and the measured value of standard spessartine and chromite (Fig. 6). Calculated using a rutile standard, Ti content in spessartine was estimated to be 3.3% less than that in the reference value, whereas the content in chromite was 2.2% higher than that in the reference. Calculations using a spessartine standard yielded over-estimates for both spessartine (+0.6%) and chromite (+6.3%), whereas calculations using a chromite standard yielded under-estimates (−6.7% for spessartine and −1.3% for chromite). Given that the Ti-in-quartz thermometer provides the minimum temperature, we selected chromite as the standard for Ti measurements, to constrain the minimum concentration.

5.2. Analytical conditions and methods for the reintegration of Ti concentration in pre-exsolution quartz

We examined a procedure to reconstruct the Ti concentration in pre-exsolution quartz. Several methods have been proposed in this regard: estimation based on chemical composition data and the area ratio of the host phase to the exsolved phase (e.g., Hokada, 2001; Raase, 1998), and estimation of a large-area-averaged chemical composition using a defocused beam (e.g., Bohlen and Essene, 1977; Harley, 1986). In the present case, exsolved rutile is less than 1 μm wide, making it difficult to calculate the area ratio. In addition, the variable length of the needles means that it is not always true that the area ratio of the rutile visible in the analyzed area is representative of the area ratio in the entire host grain. These limitations make it difficult to apply the former method for the reintegration. The large-area-averaged approach involves systematic matrix-effect errors of up to 10% (Bohlen and Essene, 1977; Raase, 1998). Taking these errors into account, we adopted the latter method due to the difficulty in applying the former method to such fine

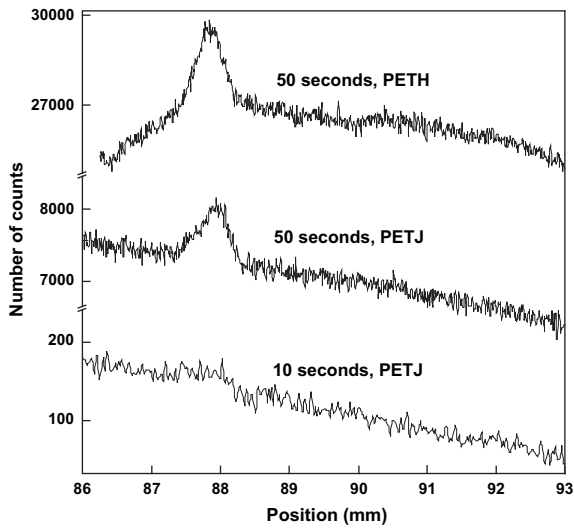


Fig. 5. X-ray spectra of quartz in OPG, as obtained by electron probe micro-analyzer (EPMA) with wavelength-dispersive X-ray analytical system (WDS) mode. PETH gives higher counts of Ti-K α (top) than does normal PET; however, a linear baseline cannot be obtained using this approach. With normal PET using a 50-s measurement at each step, a linear baseline and sufficient counts are obtained (middle); however, there is no clear Ti-K α peak for 10-s measurements (bottom).

exsolutions. To minimize the mixed-matrix effect, measurements were performed with an accelerating voltage of 25 kV to enable deeper penetration of the incident electrons into the sample. The analytical conditions were as follows: 25 kV accelerating voltage, 150 nA electron current, and 50 and 100 μm probe diameter.

5.3. Results

The Ti concentrations obtained for grains in OPG are largely independent of probe diameter (0.018–0.020 wt% on average; Fig. 7). The exsolution-free area of a quartz grain in HBG yields $\text{TiO}_2 = 0.007$ wt%, suggesting the post-exsolution Ti content. The Ti concentrations obtained for HBG with settings of 100 μm and 25 kV are 0.018 wt% on average, with a similar range in data as that obtained for OPG. The results obtained with 50 μm and 25 kV show a wide scatter (Fig. 7), indicating that a probe diameter of 50 μm is insufficient considering the 20–30 μm intervals between needles, and indicating that these results would not represent the composition throughout the entire grain.

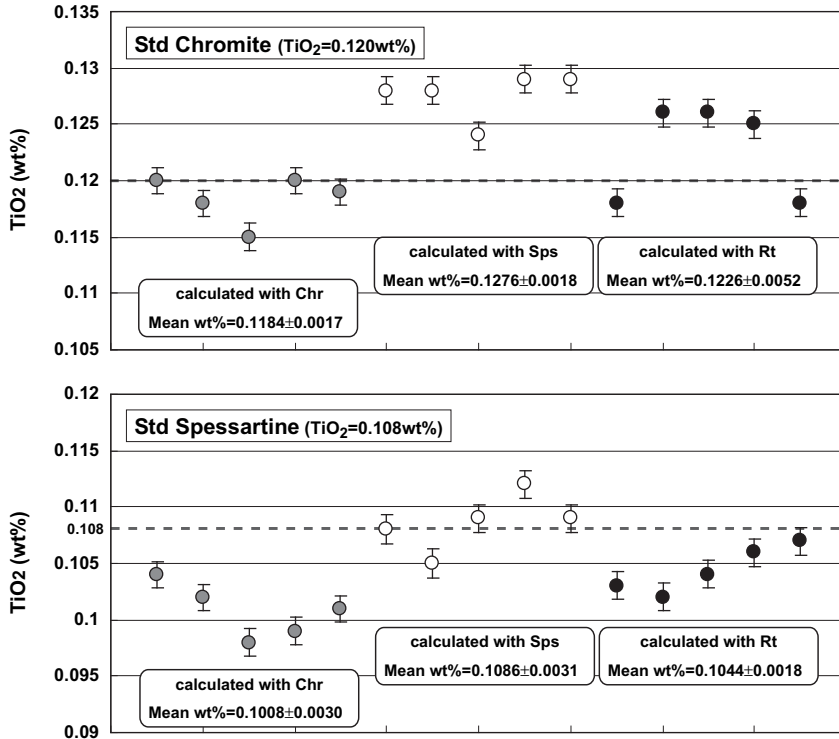


Fig. 6. Difference in the measured concentration of Ti in quartz when calibrated using three different standard materials. Dashed lines represent the reference values for the standards. Top: calibrated concentration of standard chromite. Bottom: calibrated concentration of standard spessartine.

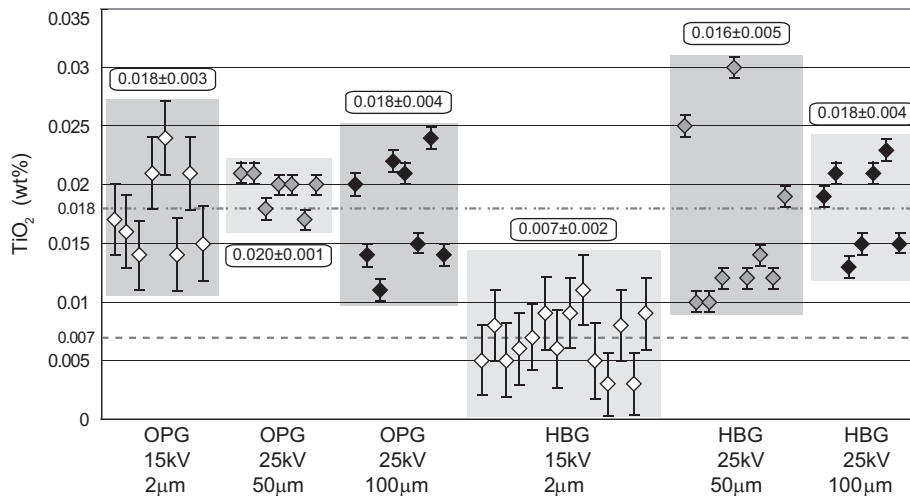


Fig. 7. Ti concentration measured using various accelerating voltages and beam diameters. Shaded boxes indicate the range of results for each setting. The values above each box are the weighted mean average of TiO_2 wt%. Chain line: average value obtained for OPG (0.018 wt%); dashed line: average value obtained for HBG with a beam diameter of 2 μm and accelerating voltage of 15 kV (0.007 wt%).

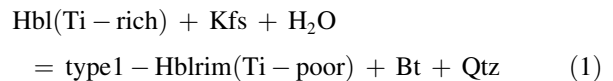
6. Discussion

6.1. Metamorphic reactions and pressure–temperature conditions

Based on mineral textures and chemistry, the mineral assemblages of OPG and HBG are interpreted as orthopyroxene + clinopyroxene + hornblende + biotite + quartz + plagioclase, and hornblende + biotite + epidote + quartz + plagioclase, respectively. The OPG sample probably records near-peak metamorphic conditions, as there is no clear evidence of retrogression. Orthopyroxene–clinopyroxene thermometers (Taylor, 1998; Wells, 1977) yield temperature conditions of 820–840 °C for OPG and HBG (Table 3), consistent with previous findings (e.g., Asami et al., 1992).

Type 1 hornblende in HBG has a near-constant X_{Mg} value from core (0.29) to rim (0.30), whereas Al_2O_3 and TiO_2 contents show significant core–rim variation (Al_2O_3 , 11.2–12.34 wt%; TiO_2 , 2.1–0.8 wt%), possibly related to cooling. Ti concentrations within the cores of type 1 hornblende in HBG are similar to those in OPG.

These observations suggest that the rims of Ti-rich type 1 hornblende (= hornblende in OPG) were replaced by Ti-poor hornblende via the following reaction:



In this reaction, the Ti in hornblende from OPG is possibly distributed in biotite. Plagioclase in HBG contains a lower proportion of K-feldspar blebs than does plagioclase in OPG, indicating consumption of the orthoclase component in plagioclase via the above reaction.

Type 2 hornblende ($X_{\text{Mg}} = 0.32$, $\text{TiO}_2 = 0.3$ wt%) has a much lower Ti content than does the rim of type 1 hornblende ($X_{\text{Mg}} = 0.30$, $\text{TiO}_2 = 0.8$ wt%), although X_{Mg} values are similar between the two types. In addition, the mode of occurrence of type 2 hornblende, which occurs as aggregates with quartz (Fig. 4b), indicates an origin via the break-down of orthopyroxene, as follows:

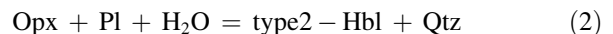


Table 3

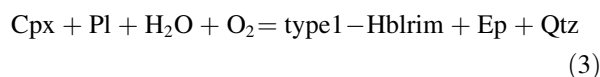
Estimated P–T conditions for felsic gneisses from the Brattnipene area, Sør Rondane Mountains.

Rock type	Pair	K	T_1 (°C)	T_2 (°C) – 5 kbar	T_2 (°C) – 10 kbar
OPG	Opx–Cpx	0.15	824	829	843
Rock type	Pair	Xab	T_3 (°C) – 5 kbar	T_3 (°C) – 10 kbar	
HBG	Hbl 1 rim–Pl	0.28	703	715	
	Hbl 2–Pl		668	677	

T_1 , Wells (1977); T_2 , Taylor (1998); T_3 , Holland and Blundy (1994).

The low Ti concentration in type 2 hornblende is consistent with an origin after orthopyroxene, which generally contains little Ti. We applied a hornblende–plagioclase thermometer (Holland and Blundy, 1994) to the rims of type 1 and type 2 hornblende, yielding equilibrium temperatures of 700–720 °C and 670–680 °C, respectively (Table 3). The rims are therefore interpreted to represent the products of intense hydration associated with intrusion of the pegmatite, and these estimated temperatures constrain the minimum temperature of the hydration event. These temperature estimates are about 100 °C higher than the previously estimated temperature of regional retrogression (580–530 °C; e.g., Asami et al., 1992).

Clinopyroxene is present in OPG but absent in HBG, which contains epidote, suggesting the following reaction:



The content of ferric iron in the rims of type 1 hornblende is higher than that in the cores, and epidote contains significant amounts of ferric iron. These observations indicate that oxygen entered the system in association with fluid infiltration. Reaction (3) might lie on the lower-pressure side of reaction curve (a) in Fig. 8, as proposed by Ellis and Thompson (1986), due to the presence of iron in epidote. Consequently, it is inferred that HBG preserves hydration conditions of around 650–700 °C and 6–8 kbar.

6.2. Temperature estimates based on Ti in quartz

Rutile exsolutions are distributed throughout the entire areas of quartz grains. If intracrystalline diffusion is effective, TiO₂ located near the grain boundary may be diffused out of the grain to form an exsolution-free rim; however, such a rim is not observed in the quartz grains from HBG, thereby indicating insignificant Ti diffusion. In addition, the bulk rock chemistry shows no significant variation in Ti concentration between OPG and HBG. Consequently, we interpret that quartz in both OPG and HBG retains its pre-exsolution Ti concentrations. Ti concentrations in homogeneous quartz in OPG are similar to reconstructed concentrations calculated for quartz in HBG that contains rutile exsolutions. This finding indicates that quartz in OPG and pre-exsolution quartz in HBG had equivalent Ti concentrations.

The Ti concentration can be converted to temperature using a Ti-in-quartz thermometer (Kawasaki and Osanai, 2008; Wark and Watson, 2006). Using the thermometer of Kawasaki and Osanai (2008), we obtain a temperature of 550 °C for the pre-hydration quartz and 440 °C for the post-hydration quartz (Table 4). This thermometer requires the analysis of Ti-saturated rutile; however, rutile is absent in both OPG and HBG, suggesting that these estimates represent minimum temperatures. The thermometer proposed by Wark and Watson (2006) is based on the degree of Ti saturation (a_{TiO_2}). Wark et al. (2007) reported that

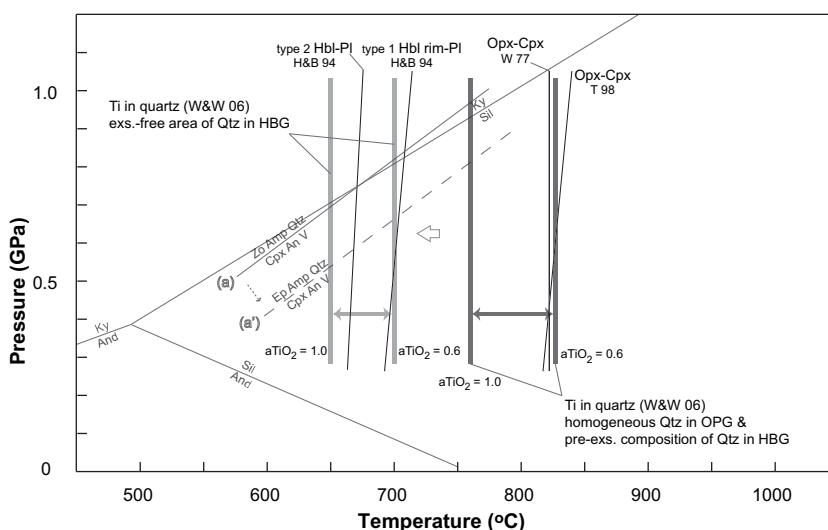


Fig. 8. Pressure–temperature conditions estimated for OPG and HBG. The dark and light grey thick lines indicate the temperature ranges estimated using a Ti-in-quartz thermometer of OPG and HBG, respectively (Wark and Watson, 2006). Reaction curve (a) is after Ellis and Thompson (1986). Temperature calibrations are as follows: H&B 94, Holland and Blundy (1994); T 98, Taylor (1998); W 77, Wells (1977).

Table 4
Measured Ti contents in quartz and T estimation with Ti-in-quartz thermometers.

Rock type	Analytical condition	Ti content (ppm)	T_1 (°C)		T_2 (°C)
			$a_{\text{TiO}_2} = 0.6$	$a_{\text{TiO}_2} = 1.0$	
OPG	2 μm , 15 kV	107	822	756	545
	100 μm , 25 kV	111	827	760	552
HBG	2 μm , 15 kV	35	686	635	439
	100 μm , 25 kV	103	817	751	543

T_1 , Wark & Watson (2006); T_2 , Kawasaki and Osanai (2008).

felsic rocks have an a_{TiO_2} value of 0.6–1.0 in the presence of a Ti-rich phase such as ilmenite or titanite. In the present study, ilmenite is present instead of rutile in both OPG and HBG; therefore, values of 0.6–1.0 were applied.

Using the method of Wark and Watson (2006), we obtained temperatures of 830 °C ($a_{\text{TiO}_2} = 0.6$) to 760 °C ($a_{\text{TiO}_2} = 1.0$) for homogeneous quartz in OPG, and 820 °C ($a_{\text{TiO}_2} = 0.6$) to 750 °C ($a_{\text{TiO}_2} = 1.0$) for the reconstructed pre-exsolution quartz composition in HBG, which is interpreted as the pre-hydration temperature. These values are consistent with estimates obtained using orthopyroxene–clinopyroxene thermometers (820–840 °C) for OPG. An exsolution-free portion of a quartz grain in HBG yields a temperature of 690 °C ($a_{\text{TiO}_2} = 0.6$) to 640 °C ($a_{\text{TiO}_2} = 1.0$), which is interpreted as the temperature during the hydration event, consistent with the temperature obtained using the hornblende–plagioclase thermometer (670–720 °C) for HBG (Table 4 and Fig. 8).

The retrogression event had a marked effect on the chemical composition of hornblende and plagioclase; however, the reconstructed pre-exsolution quartz composition in HBG is probably a near-peak temperature. This indicates that the Ti-in-quartz thermometer has the advantage of being able to estimate the peak metamorphic temperature from intensely retrogressed samples.

6.3. Implications for rutile exsolution in HBG

The mechanism of exsolution is generally controlled by the degree of super-saturation, which in turn is related mainly to cooling. In the case of the studied samples, the rutile-exsolution-free quartz in OPG and the rutile-exsolution-bearing quartz in HBG are thought to have experienced the same pressure-temperature-time path. Moreover, Ti concentrations are similar in quartz from both OPG and HBG. The main difference between OPG and HBG is that

the former shows little evidence of hydration, whereas the latter experienced intense hydration during cooling. These observations suggest that intense hydration may play a role in triggering the nucleation of rutile lamellae, and thereby the occurrence of rutile exsolution. Although the mechanism of nucleation of the lamellae, driven by hydration, is beyond the scope of this paper, we note two ways in which hydration might influence nucleation: hydration results in an increase in the degree of super-saturation, or a retrograde reaction within HBG involved quartz. We found a wide distribution of rutile exsolution in quartz across a large part of the Northeastern Terrane of the Sør Rondane Mountains (Fig. 1). If retrograde hydration is related to the occurrence of exsolution, the widespread distribution of exsolved rutile may indicate the extent of large-scale high-grade (granulite facies?) metamorphism and subsequent hydration.

Given that rutile exsolution has been reported in several minerals from ultra-high pressure and/or ultra-high temperature metamorphic terranes, these textures could be indicative of such extreme conditions (e.g., Osanai et al., 2001; Zhang et al., 2003). However, in the present study, rutile exsolution occurred in quartz during a temperature drop from <850 °C to 650–700 °C. This finding suggests that ultra-high temperature is not essential for the development of rutile exsolution in quartz.

7. Conclusions

1. Rutile exsolution in quartz was found in retrograde hornblende-biotite gneiss derived (bleached) from orthopyroxene felsic gneiss.
2. The compositions of orthopyroxene and clinopyroxene in OPG indicate a temperature of 840 °C, interpreted as the near-peak temperature. The compositions of hornblende and plagioclase in HBG suggest temperatures of 670–700 °C, interpreted as the temperature of the hydration event.

3. Ti concentrations in quartz were 110 ppm (equivalent to 760–820 °C) for homogeneous quartz in OPG and 35 ppm (650–700 °C) for an exsolution-free area in quartz within HBG. The pre-exsolution Ti concentration in quartz within HBG is 103 ppm, similar to the value in homogeneous quartz within OPG.
4. Although the main constituent minerals in HBG record the conditions of the hydration event, the reconstructed Ti content in pre-exsolution quartz within HBG records pre-hydration conditions. Thus, the Ti-in-quartz thermometer has the potential to be a powerful tool in reconstructing the history of metamorphic rocks modified by retrogression.

Acknowledgments

We would like to express our sincere thanks to the members of the 48th and 49th Japan Antarctic Research Expeditions (JARE), and the crew of the icebreaker *Shirase*. T.A. acknowledges Profs. Y. Motoyoshi and K. Shiraishi for enabling him to participate in JARE. We greatly appreciate the constructive reviews and suggestions of two anonymous reviewers. The cost to T.A. of conducting field work in Antarctica was offset in part by grants-in-aid from the Graduate University for Advanced Studies and the Japan Polar Research Association.

References

- Asami, M., Osanai, Y., Shiraishi, K., Makimoto, H., 1992. Metamorphic evolution of the Sør Rondane Mountains, East Antarctica. In: Yoshida, Y., Kaminuma, K., Shiraishi, K. (Eds.), *Recent Progress in Antarctic Earth Science*. Terra, Tokyo, pp. 7–15.
- Asami, M., Shiraishi, K., 1987. Kyanite from the western part of the Sør Rondane Mountains, East Antarctica. *Proc. NIPR Symp. Antarctic Geosci.* 1, 150–168.
- Bohlen, S.R., Essene, E.J., 1977. Feldspar and oxide thermometry of granulites in the Adirondack Highlands. *Contrib. Mineral. Petrol.* 62, 153–169.
- Ellis, D.J., Thompson, A.B., 1986. Subsolidus and partial melting reactions in the quartz excess CaO + MgO + Al₂O₃ + SiO₂ + H₂O system under water-excess and water-deficient conditions to 10 kbar: some implications for the origin of peraluminous melts from mafic rocks. *J. Petrol.* 27, 91–121.
- Harley, S.L., 1986. A sapphirine–cordierite–garnet–sillimanite granulite from Enderby Land, Antarctica: implications for FMS petrogenetic grids in the granulite facies. *Contrib. Mineral. Petrol.* 94, 452–460.
- Hokada, T., 2001. Feldspar thermometry in ultrahigh-temperature metamorphic rocks: evidence of crustal metamorphism attaining ~1100 °C in the Archean Napier Complex, East Antarctica. *Am. Mineral.* 86, 932–938.
- Holland, T., Blundy, J., 1994. Non-ideal interactions in calcic amphiboles and their bearing on amphibole–plagioclase thermometry. *Contrib. Mineral. Petrol.* 116, 433–447.
- Jacobs, J., Bauer, W., Fanning, C.M., 2003. Late Neoproterozoic/Early Paleozoic events in central Dronning Maud Land and significance for the southern extension of the East African Orogen into East Antarctica. *Precam. Res.* 126, 27–53.
- Kawasaki, T., Motoyoshi, Y., 2007. In: Cooper, A., Raymond, C. (Eds.), *Antarctica: A Keystone in a Changing World*. US Geological Survey Open-File Report 2007-1047. Solubility of TiO₂ in garnet and orthopyroxene: Ti thermometer for ultra high temperature granulites. doi:10.3133/of2007-1047.srp038 Short Research Paper 038.
- Kawasaki, T., Osanai, Y., 2008. Empirical thermometer of TiO₂ in quartz for ultrahigh-temperature granulites of East Antarctica. In: Satish-Kumar, M., Motoyoshi, Y., Osanai, Y., Hiroi, Y., Shiraishi, K. (Eds.), *Geodynamic Evolution of East Antarctica: A Key to the East–West Gondwana Connection*. Geological Society, London, Special Publication 308, pp. 139–146.
- Kojima, S., Shiraishi, K., 1986. Note on the geology of the western part of the Sør Rondane Mountains, East Antarctica. *Memoir Nat. Inst. Polar Res., Special Issue* 43, 116–131.
- Kretz, R., 1983. Symbols for rock-forming minerals. *Am. Mineral.* 68, 277–279.
- Leake, B.E., Woolley, A.R., Arps, C.E.S., Birch, W.D., Gilbert, M.C., Grice, J.D., Hawthorne, F.C., Kato, A., Kisch, H.J., Krivovichev, V.G., Linthout, K., Laird, J., Mandarino, J.A., Maresch, W.V., Nickel, E.H., Rock, N.M.S., Schumacher, J.C., Smith, D.C., Stephenson, N.C.N., Ungaretti, L., Whittaker, E.J.W., Youzhi, G., 1997. Nomenclature of amphiboles: report of the subcommittee on Amphiboles of the International Mineralogical Association, Commission on New Minerals and Mineral Names. *Can. Mineral.* 35, 219–246.
- Osanai, Y., Shiraishi, K., Takahashi, Y., Ishizuka, H., Tainosho, Y., Tsuchiya, N., Sakiyama, T., Kodama, S., 1992. Geochemical characteristics of metamorphic rocks from the central Sør Rondane Mountains, East Antarctica. In: Yoshida, Y., Kaminuma, K., Shiraishi, K. (Eds.), *Recent Progress in Antarctic Earth Science*. Terra, Tokyo, pp. 17–27.
- Osanai, Y., Toyoshima, T., Owada, M., Tsunogae, T., Hokada, T., Crowe, W.A., Kusachi, I., 2001. Ultrahigh temperature sapphirine–osumilite and sapphirine–quartz granulites from Bunt Island in the Napier Complex, East Antarctica–Reconnaissance estimation of *P–T* evolution. *Polar Geosci.* 14, 1–24.
- Osanai, Y., Yoshimura, Y., 2002. High-temperature limit of crustal metamorphism: a perspective of ultra-high temperature metamorphism. *Chishitsu News* 573, 10–26 (in Japanese).
- Raase, P., 1998. Feldspar thermometry: a valuable tool for deciphering the thermal history of granulite-facies rocks, as illustrated with metapelites from Sri Lanka. *Can. Mineral.* 36, 67–86.
- Seno, K., Ishizuka, H., Motoyoshi, Y., Shiraishi, K., 2002. Quantitative chemical analyses of rocks with X-ray fluorescence analyzer: (3) Rare earth elements. *Ant. Rec.* 46, 15–33 (in Japanese with English abstract).
- Shiraishi, K., Dunkley, D.J., Hokada, T., Fanning, C.M., Kagami, H., Hamamoto, T., 2008. Geochronological constraints on the Late Proterozoic to Cambrian crustal evolution of eastern Dronning Maud Land, East Antarctica: a synthesis of SHRIMP U–Pb age and Nd model age data. In: Satish-Kumar, M., Motoyoshi, Y., Osanai, Y., Hiroi, Y., Shiraishi, K. (Eds.), *Geodynamic Evolution of East Antarctica: A Key to the East–West Gondwana Connection*. Geological Society, London, Special Publication 308, pp. 139–146.
- Shiraishi, K., Kagami, H., 1992. Sm–Nd and Rb–Sr ages of the metamorphic rocks from the Sør Rondane Mountains, East

- Antarctica. In: Yoshida, Y., Kaminuma, K., Shiraishi, K. (Eds.), *Recent Progress in Antarctic Earth Science*. Terra, Tokyo, pp. 29–35.
- Shiraishi, K., Kojima, S., 1987. Basic and intermediate gneisses from the western part of the Sør Rondane Mountains, East Antarctica. *Proc. NIPR Symp. Antarctic Geosci.* 1, 129–149.
- Shiraishi, K., Osanai, Y., Ishizuka, H., Asami, M., 1997. Geological map of the Sør Rondane Mountains, Antarctica. *Antarctic Geological Map Series, Sheet 35, Scale 1:250 000*. National Institute of Polar Research, Tokyo.
- Taylor, W.R., 1998. An experimental test of some geothermometer and geobarometer formulations for upper mantle peridotites with application to the thermobarometry of fertile lherzolite and garnet websterite. *Neues Jahrbuch für Mineralogie-Abhandlungen* 172, 381–408.
- Wark, D.A., Hildreth, W., Spear, F.S., Cherniak, D.J., Watson, E.B., 2007. Pre-eruption recharge of the Bishop magma system. *Geology* 35, 235–238.
- Wark, D.A., Watson, E.B., 2006. TitaniQ: a titanium-in-quartz geothermometer. *Contrib. Mineral. Petrol.* 152, 743–754.
- Wells, P.R.A., 1977. Pyroxene thermometry in simple and complex systems. *Contrib. Mineral. Petrol.* 62, 129–139.
- Zhang, R.Y., Zhai, S.M., Fei, Y.W., Liou, J.G., 2003. Titanium solubility in coexisting garnet and clinopyroxene at very high pressure: the significance of exsolved rutile in garnet. *Earth Planet. Sci. Lett.* 216, 591–601.

